3D printing implants for fracture healing studies in rats

Malcolm Horal

2015

LUND
UNIVERSITY

Bachelor's Thesis in

Biomedical Engineering

Faculty of Engineering LTH
Department of Biomedical Engineering

supervised by

Hanna Isaksson

Abstract

The purpose of this project was to investigate the possibility to create 3D printed implants intended for bone healing studies in small animals at the Biomechanics group at Lund University. The aim was to use cheaper but stable non metallic implants and find out what printers and materials are suitable and accessible today. An *Ultimaker 2* was used to produce both nails and screws in Polyhydroxyalkanoates (PHA) and Polylactic acid (PLA) and Nylon which were analyzed both qualitatively and quantitatively. A three point bending test and the effect subjecting them to a wet and warm environment was investigated.

It was found that the produced nails were adequate but it was not possible to produce the screws with satisfactory results with this specific printer. The samples made out of Nylon were generally not strong enough and lost too much stiffness when immersed in saline. The quality of the produced samples varied, and manual polishing was required to achieve the desired results. The PLA/PHA samples were stiff enough even after being immersed in saline. It was concluded that it is too early to start using 3D printing with this type of printer for in vivo studies.

Keywords-*3D printing, implants, PHA, PLA*

Contents

1 Introduction & Background

Fracture healing is a complex biological process. Despite today's knowledge and technology, 5-10% of all fractures are either nonunion or delayed [1]. The phenomena of non-healing is especially occurring in older patients, hence effective treatments of fractures in these patients are essential. The research at the Biomechanics and Orthopaedics research groups at Lund University use animal models of fracture healing to develop methods that can better assess bone quality and fracture healing [2, 3]. Most nails and screws used today are made out of metal and they are neither cheap nor customizable. This restrains the research both economically and in terms of limiting the use of equipment to what is available on the market.

Three different models are used for studies on bone healing in rats. The bone screw/chamber, the fracture healing model and the critical defect model. The evaluation methods include mechanical testing (e.g. three point bending), micro-Computer Tomography (micro CT), Positron Emission Tomography, Small-Angle X-ray Scattering, Fourier Transform Infrared Spectroscopy, Energy Dispersive Spectroscopy and Scanning Electron Microscopy [4].

The bone screw and bone chamber screw model are found left of figure 1. Pull or torque tests are performed to measure ingrowth of bone tissue at the bone screw. Bone generation in the stress isolated cavity is measured in the chamber screw [5]. The two other models are of fracture healing types where an intramedullary nail is inserted in the femur. For a normal fracture a 1.1 mm thick K-wire [6] is used, as seen in the middle of figure 1. For critical defects a RatNail from manufacturer RISystems [7] is inserted as seen to the right in figure 1. Using metal implants can be problematic when analyzing the results.

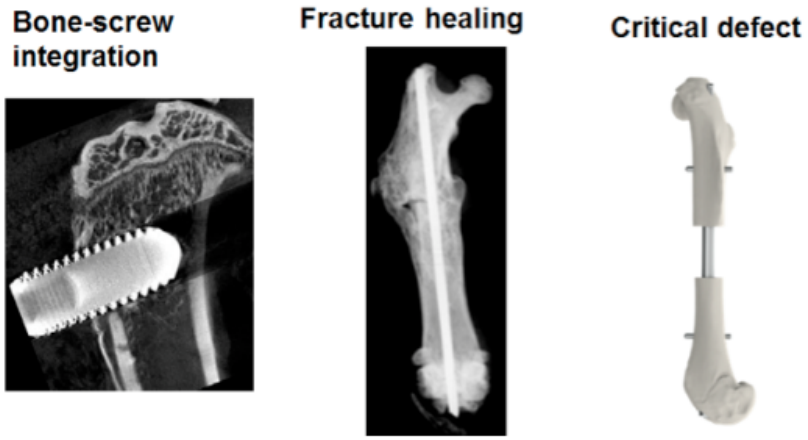

Figure 1: Images of the three models used for bone healing studies. From left to right: bone-screw, fracture healing and critical defect.

Some of the imaging technologies, especially the most commonly used micro CT, are not capable of obtaining detailed images of tissues in absolute proximity of metal because of interference generated by the metal object.

1.1 3D Printing

The use of 3D printing technology has increased rapidly the last years [8–10]. Within medical engineering it gives the possibility to effectively manufacture customized structures at a low cost depending on the patients' specific needs [10, 11].
3D printing is not one but a group of many technologies. One of those technologies is Fused Deposition Modeling (FDM). FDM has been around since the '80s and it's found in nearly all consumer level printers today [12]. FDM works by melting a material and extruding it through a heated extrusion head or nozzle. When the material cools down it hardens. The structure is created one layer at a time [13]. Normally a

thermoplastic material, referred to as filament, is used. Common filaments used for manufacturing include polymers Acrylonitrile Butadiene Styrene (ABS), Polycarbonates (PC), PHA and PLA to name a few [13]. The filament is often wound on a coil which unreels when fed through the nozzle to supply material to the structure being manufactured. Steppers or servo motors moves the nozzle and adjust the flow of the filament. The nozzle can be moved in the horizontal and vertical plane. The mechanism is typically controlled by a computer-aided manufacturing software package running on a micro controller.

Recently more materials, blends and hybrids have been introduced for FDM printers. The mixture PLA/PHA and its separate components are relatively cheap, biocompatible and the blend is slightly tougher than pure PLA. Nylon is a tough material which is commonly used in the medical field, e.g. for surgical suture [14].

2 Aim

The aim of this study was to investigate the possibilities of 3D printing non metallic implants for animal studies of bone healing. The aim was to find out what printers and materials are available and suitable by mechanically investigate the effect of a three point bending test on samples and analyze the effect of the samples being subjected to a wet environment.

Furthermore the study aimed at gathering experience to evaluate whether 3D printing is a suitable approach for the biomechanics and orthopaedics research groups in the near future.

3 Method

The first step was to do a literature study and online research. Also a visit to *indistrimässan*, an industry convention, in Malmö was done to find information about what kind of 3D printing was suitable for this project and what was available in the vicinity of Lund.
Secondly 3D models of the implants were created. Nails were created so that both quantitative and qualitative properties could be tested. Screws were created to qualitatively determine the printers limits and possibilities. Lastly pellets were created to be immersed in saline to see how the material would withstand a moist environment for a longer period.

3.1 Design

The implants used in the study, seen in figures 3–5, were modeled in *Fusion360* according to measurements and schematics. Further details on all dimension can be found in Appendix A.

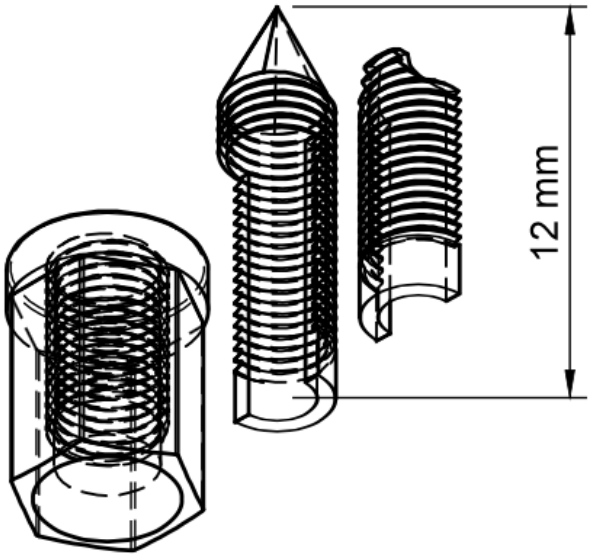

Figure 2: A schematic of the shielded bone screw. The two rightmost pieces are put together and inserted in the nut housing, left. This leaves two openings to the stress isolated cavity where bone is supposed to form.

3.2 3D Printing

An *Ultimaker 2* by *Ultimaker* was used for manufacturing. A new interchangeable nozzle system, *The Olsson Block*, was installed in the printer to support nozzle diameters of 0.25, 0.4 and 0.8 mm. Recommendations and "trial and error" was used to qualitatively determine the best settings for the printer.

The 3D models were sliced automatically with Cura (*v15.02.1* for OSX) and printed one at a time. Two nail diameters were printed, 1.1 mm and 1.5 mm. PLA nails were printed at 210° C, build plate temperature at 60° C, at 15 mm/s. For the 0.25 nozzle 0.02 mm layer height was chosen and for the 0.4 nozzle 0.04 mm was used. The PLA/PHA blend, from manufacturer *ColorFabb*, used is slightly tougher than pure PLA with a

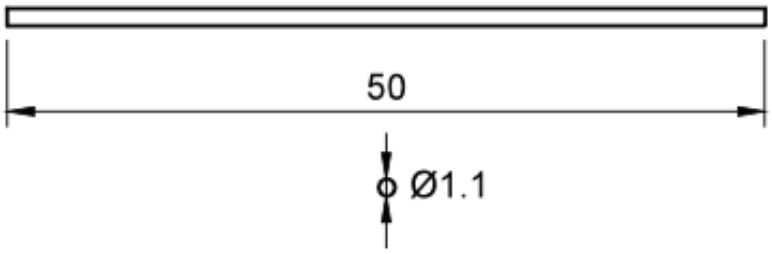

Figure 3: A schematic of the intramedullary nail. A ⌀1.5 mm version was also created

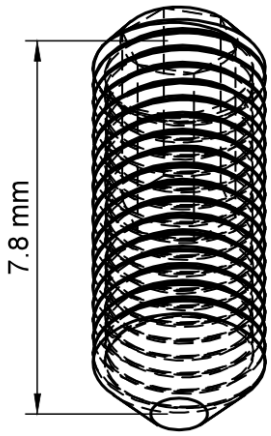

Figure 4: A schematic of the bone screw.

Young's modulus of 3.0 GPa [15, 16]. In comparison, a rat femur has the Young's modulus of around 1.5–3.4 GPa under bending [17, 18]. Nylon nails were printed with the 0.4 mm nozzle installed at 245° C, build plate temperature was 60° C. The Nylon was of the Bridge-type from manufacturer *Taulman 3D* with a Young's modulus of 190 MPa [19]. Further details on manufacturing settings can be found in tables 5–4 in Appendix B.

Based on printing settings, materials and diameter variations 20 samples were created and divided into 7 groups, described in table 1. Each group contained three samples (except for group

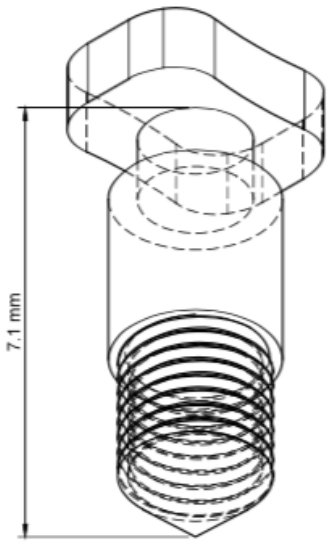

Figure 5: A schematic of the torque screw.

5 which only contained two samples). Groups 1–4 and 6–7 were printed according to the settings mentioned above. The samples in group 5 were manually extruded hanging through a 0.8 mm nozzle at 200° C. All nails were stored dry in room temperature after printing. Nails in groups 4 and 7 were later transfered to saline containers 24 hours prior to the three point bending test. The diameter of each nail was measured with a caliper near the middle in quadruplicates and they were then microphotographed from the top, side and bottom.

3.3 Three point bending

The samples were subjected to a three point bending test in a mechanical testing jig (Instron 8511 load frame, High Wycombe, UK / MTS test suite controller with three point bending configuration). Group 4 and 7 were put into saline for 24 hours prior to the test. Group 1 to 5 were preloaded at 0.1 mm/s to 1 N to ensure the contact surfaces were properly

Table 1: Manufactured samples divided into groups depending on treatment, material and diameter variations.

Group	Number	Material	Model ⌀	Nozzle ⌀	Storage
1	3	PLA	1.1 mm	0.4 mm	Dry
2	3	PLA	1.5 mm	0.4 mm	Dry
3	3	PLA	1.1 mm	0.25 mm	Dry
4	3	PLA	1.1 mm	0.4 mm	Saline
5	2	PLA	-	0.8 mm	Dry
6	3	Nylon	1.1 mm	0.4 mm	Dry
7	3	Nylon	1.1 mm	0.4 mm	Saline

aligned and no sliding of the sample occurs. The samples were held for 10 seconds before being loaded at 0.1 mm/s until breakage for 6 mm. Breakage was defined as a 20% drop in force between two measurements. For samples in group 6 the preload limit was changed to 0.4 N and the main loading continued for a maximum of 10 mm. For samples in group 7 the preload limit was changed down to 0.25 N and main loading was kept at 10 mm maximum. Force displacement curves were recorded for all samples. Young's modulus was calculated in region **A** of figure 6. It was chosen as the interval from a tenth to a third of the data points until reaching the point corresponding to the maximum force. This interval was visually revised to be sure any "initial turbulence" and data after the yield point **B** was excluded from the calculations [20].

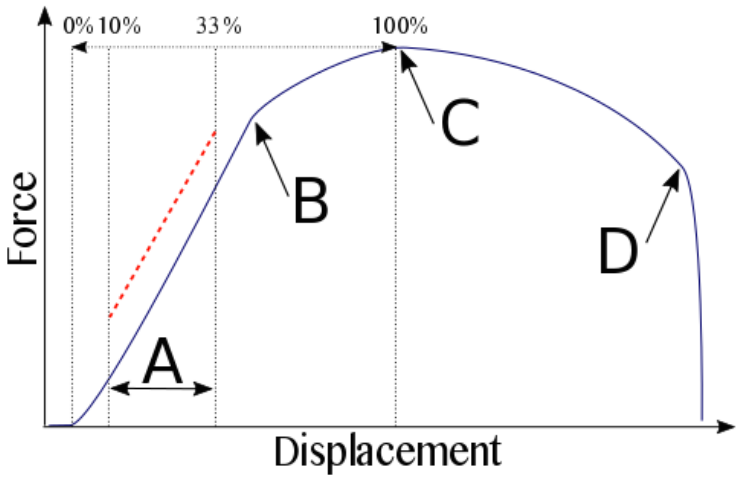

Figure 6: Interval **A** shows the elastic region used for the calculations. **B** is the yield point. **C** is the point of Maximum force. **D** is the fracture point.

3.4 Material Degradation

The effect on a foreign PLA/PHA object entering the body was analyzed by putting PLA/PHA pellets in test tubes with saline. This was done to see if any biodegradation via hydrolysis would occur [21]. The pellets were printed six at a time at 180°, 200° and 220° C to examine if the printing temperature affects PLA polymer X-linking and degradation of the PLA chains [21]. The 18 pellets (⌀5 mm, height 2 mm) were divided into 6 groups with 3 samples depending on manufacturing and incubation temperature. They were put in separate test tubes with 10 ml of saline and were then incubated. To mimic body temperature, 37° C was used and to accelerate an eventual process the samples was exposed at 60° C. They were weighted after 0, 2, 6 and 15 weeks. Prior to weighing, the pellets were dried at 60° C for 24 hours. The tubes were emptied and refilled with new saline after every weighing so that a possible degradation would

not buffer the solution. A picture of pellets in the drying and scaling process can be seen in figure 7.

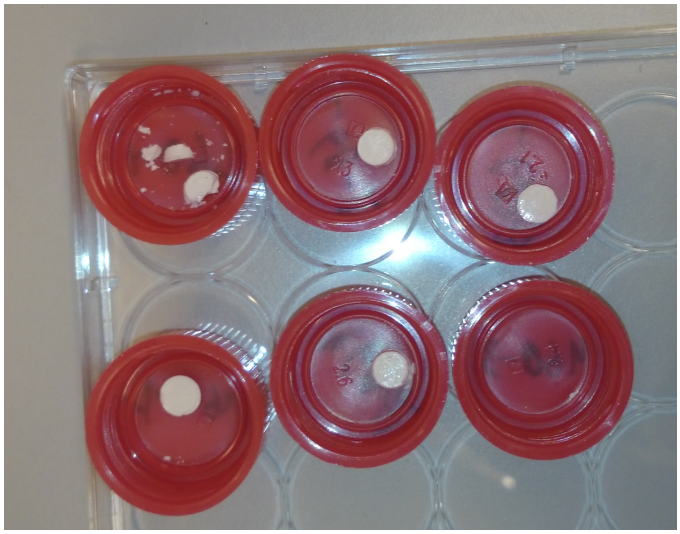

Figure 7: Pellets dried and prepared before weighing. The pellet the in the upper left corner has been chipped as an effect of degradation and handling.

3.5 Screws

All screws, seen in figures 2, 4 and 5 were printed with the 0.25 mm nozzle and the same settings as the nails in group 3 (table 3 in Appendix B) with the only difference that a brim was printed instead of a raft.

4 Results

4.1 Nail diameter

The diameter measurements can be seen in figure 8. A full data sheet can be found in Appendix C.

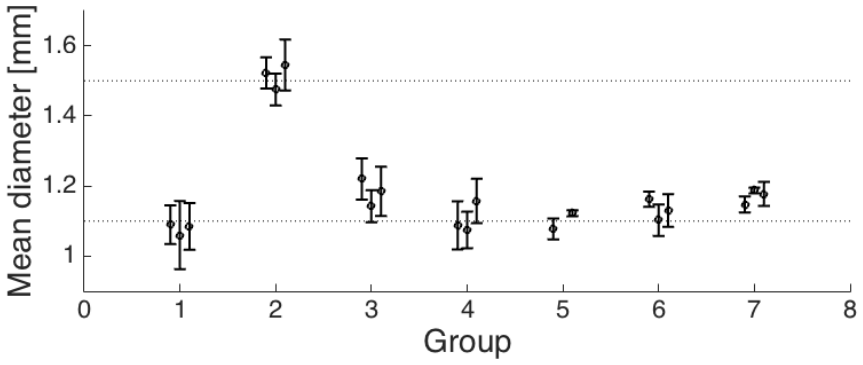

Figure 8: Mean diameter for all 20 separate samples in 7 groups as described in detail in table 1.

4.2 Microphotography

Microphotographs of the nails with different nozzle and structure diameter are found in figures 9–11. Photographs were taken, in accordance to the manufacturing set up, from the top side, bottom side and from the side of the nail. The nails run left to right in the pictures and the vertical line marks 100 μm. More photos are found in figures 21–23 in Appendix E.

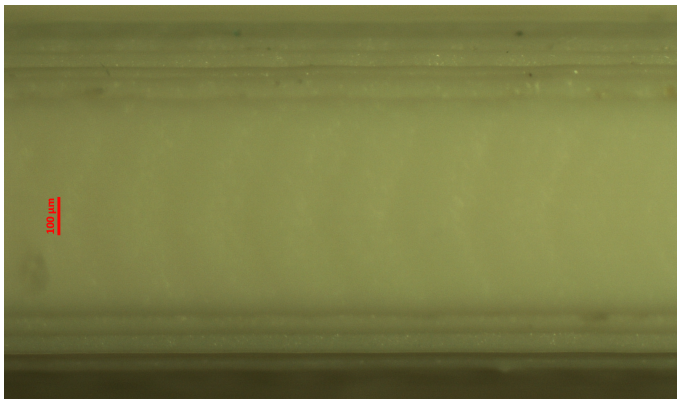

Figure 9: Microscopy of PLA nail top side with ⌀1.1 mm printed with the ⌀0.4 mm nozzle from group 1.

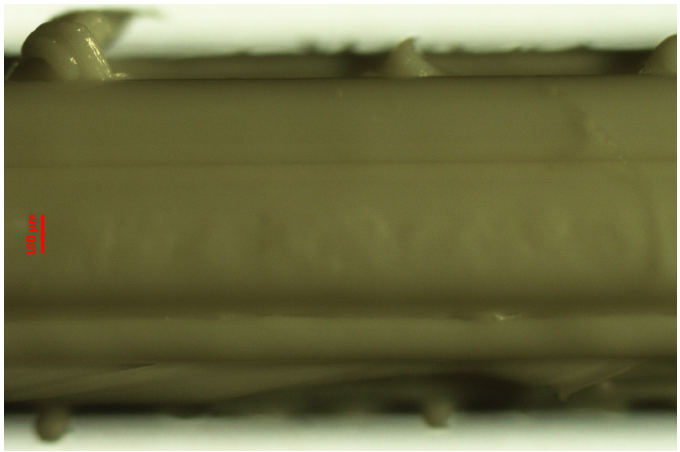

Figure 10: Microscopy of PLA nail bottom with ⌀1.1 mm printed with the ⌀0.4 mm nozzle from group 1.

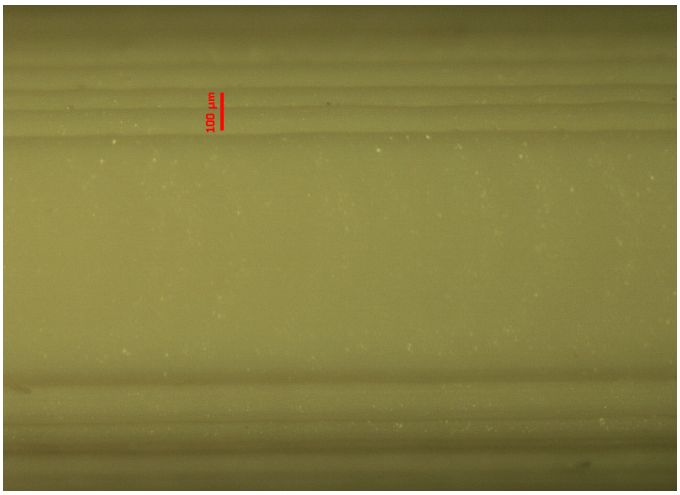

Figure 11: Microscopy of PLA nail top side with ⌀1.5 mm printed with the ⌀0.4 mm nozzle from group 2.

4.3 Screws

Images of produced screws are seen in 12.

Figure 12: From left to right: Bone chamber screw, three pieces. Bone screw and torque screw.

4.4 Three point bending

Graphs 13 and 14 shows the Force-displacement curves of the three point bending test for the PLA and Nylon samples respectively. Group individual curves can be found in figures 24–30 in Appendix F.
Mean Maximum force for every group are seen in figure 15. Figure 16 shows the mean Youngs's modulus for every group.

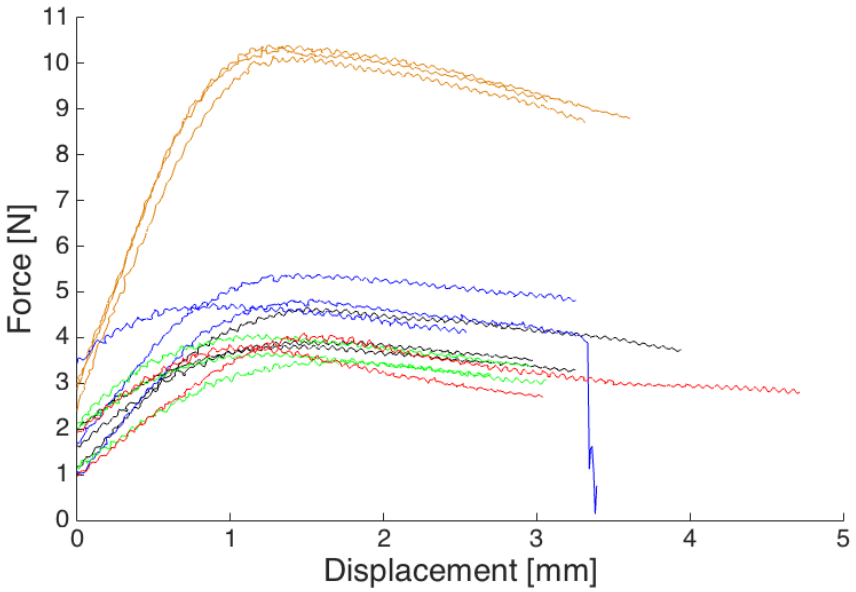

Figure 13: Force-displacement curve of PLA samples. Black: group 1. Brown: group 2. Blue: group 3. Green: group 4. Red: group 5. Groups are described in detail in table 1.

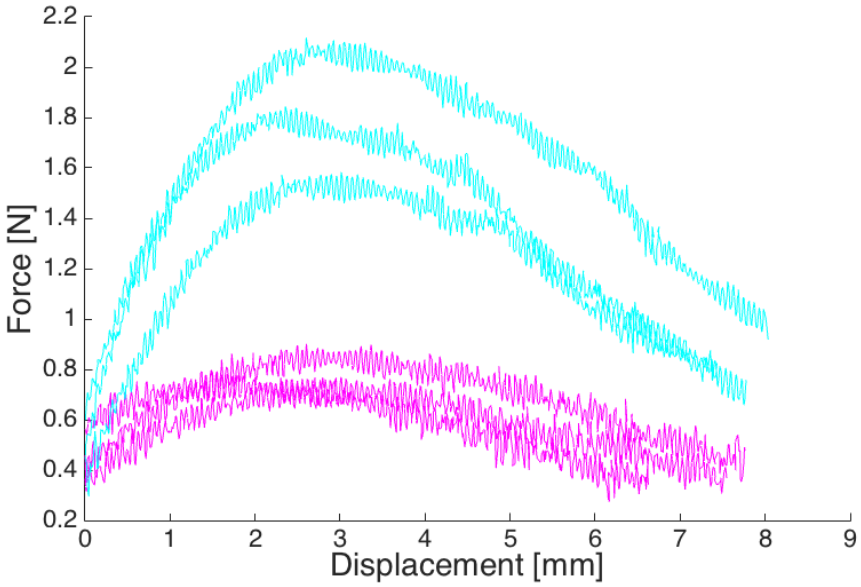

Figure 14: Force-displacement curve of Nylon samples. Magenta: group 6. Cyan: group 7. Groups are described in detail in table 1

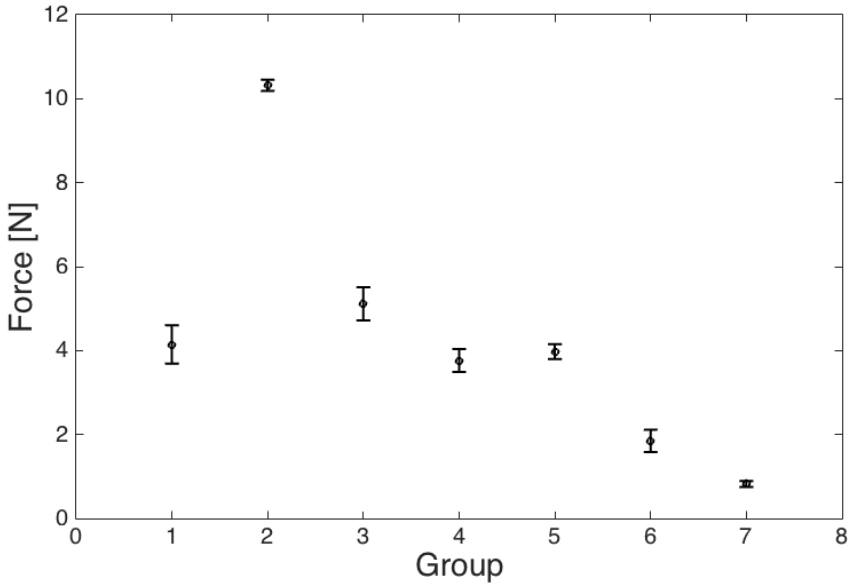

Figure 15: Mean maximum force applied during three point bending test to all nails in all 7 groups as described in detail in table 1.

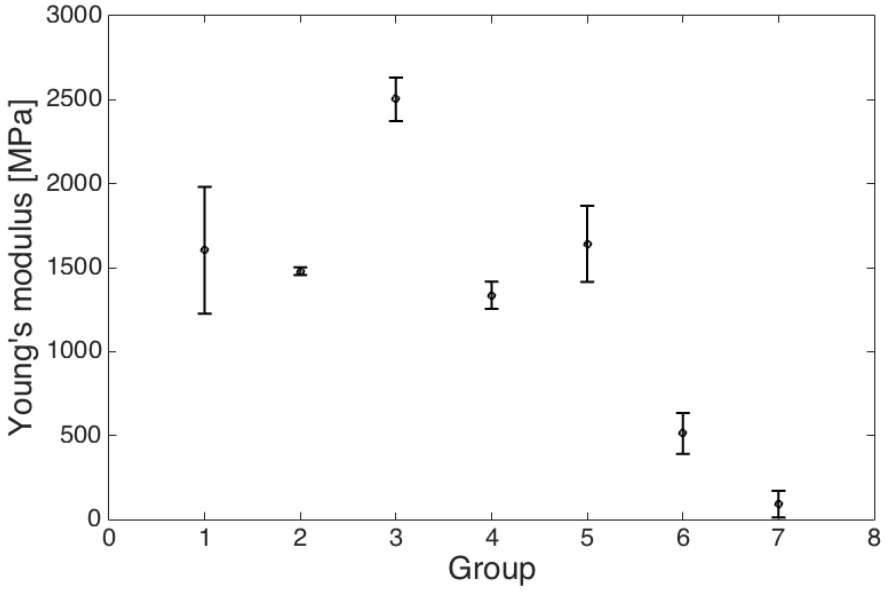

Figure 16: Mean Young's modulus for all 7 nail groups as described in detail in table 1.

4.5 Material degradation

Material degradation over time is found in figure 17.

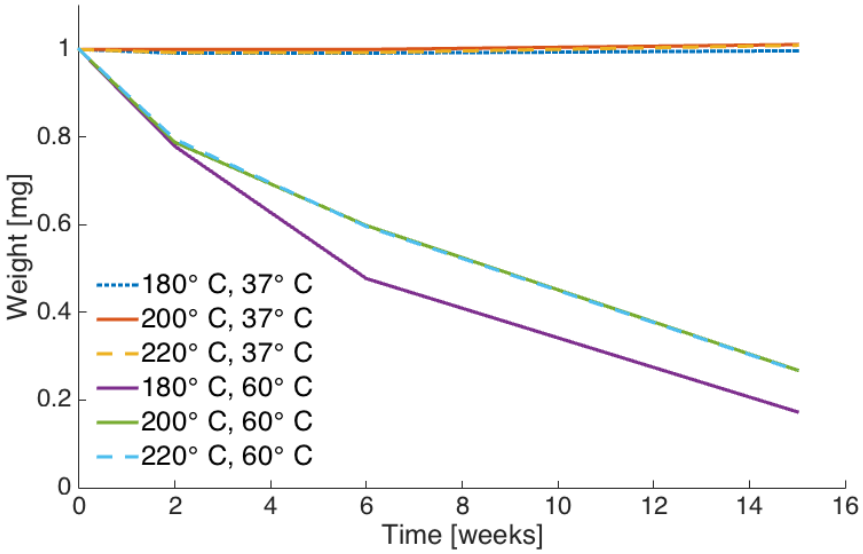

Figure 17: Mean material degradation over 15 weeks for PLA/PHA produced in 180°, 200° and 210° C kept in saline at 37° and 60° C.

5 Discussion

Regarding the diameter data we see that it was hard to get a consistent result. Printing the larger diameter and using the ⌀0.4 mm nozzle seems to be better in regards to achieving the nail diameter aimed at. Reverse engineering could be used to change the size of the 3D model so that the desired diameter of the nails is achieved. Extruding manually through a ⌀0.8 mm nozzle performed satisfactory in the two cases. This manufacturing method contained manual elements to such an extent that the reproducibility can be questioned.

The first thing to consider regarding the microscopy images are the clearly visible defects in figure 10. Those knobs were around a tenth of the whole nail diameter. The limitation of the printing resolution because of the nozzle diameter and resolution in the vertical axis is clearly visible in the top view in figures 21 and 23. The samples were manually separated from the raft with a scalpel. This process could be improved further, or automatized to reduce the irregularities on the underside. With these results it is fairly reasonable to make the assumption that the nails are not perfectly round.

Regarding the screws in figure 12 the results were not satisfactory in regards to the overall structure compared to the CAD models 3–5. Various attempts to find optimal settings were made without success. Some samples could be considered acceptable, whilst next batch yielded unsatisfactory results. Using a 3D printer with higher resolution would obviously improve the quality. Optimizing the settings even further through trial and error could have yielded better results but probably not good enough. Since slicing is an automated process done by the software, removing the threads from the models (and leave it to post processing) may help as well. This could minimize the risk of the software choosing a "bad" paths adjusted to the very small differences due to the threads.

In the three point bending test it was clear that the protocol used was not optimal. Only one curve reached the fracture point. This meant that energy and toughness could not be calculated and therfore material and structure information was lost. Concerning the force-displacement results a considerable part of the the elastic region for nail 3, group 3, (see Appendix F figure 26) and nail 2, group 7, (see Appendix F figure 30) were cut off. They were excluded from the calculations in results for group 3 and 7 in figure 16, and the selection fell with a third, which yields a somewhat distorted value of the mean

and SD values. The curves for the Nylon samples has distinct noise factor which quite possibly was a combined result of the magnitude of the data and the sensitivity of the equipment. The magnitude could also explain the low SD for group 2, seen in figure 16 (and 25 in Appendix F). A thicker sample gives a better result, regarding almost all aspects. It would have been preferable to use more samples to better evaluate the experiments. A clear distinction in performance is seen between the PLA and Nylon samples. Keeping the PLA in saline for 24 hours prior to the bending test did not alter the stiffness. Nylon on the other hand drastically lost its stiffness when kept in saline.

Dry PLA and Nylon structures seem to maintain the stiffness of the material [15]. This means that the manufacturing process does not have a major effect on the material properties. The PLA nails was stiffer then nails made out of Nylon, which is to be expected.

Different printing temperatures does not seem to have a effect on the rate of material degradation at all. In figure 17 one can see that the saline environment does not affect the samples incubated at 37° C but noticeable changes appear when they were kept at 60° C. The sample in the upper left corner of figure 7 (sample 1 kept at 60° C, printed at 180° C) was broken into pieces. Also sample 2, kept at 60° C, printed at 220° C got chipped along the edges. Many of the other samples kept at 60° C were chipped when handled with the forceps which affects the result. This makes it safe to assume that PLA/PHA structures would not degrade because of the warm and salty environment in an animal study that runs up to 15 weeks.

6 Conclusion

To make 3D printing of implants a viable reality for animal studies, some details must be further investigated. A printer with higher resolution must be tested and a method for assuring even quality throughout different print batches should be found. Finally the whole process must be performed in a sterile environment so that the materials could be tested and later used in vivo.

7 Acknowledgements

I take this opportunity to express my gratitude to all of the people who have helped me throughout my work with this thesis: Associate Professor Hanna Isaksson, Department of Biomedical Engineering, for her help, encouragement and feedback as my supervisor. Associate Professor Mikael Evander, Department of Biomedical Engineering, my supervisor in the 3D workshop who help me in the workshop. PhD Deepak Raina, Department of Orthopaedics, for teaching me about chemistry. Biomedical Scientist, Mea Pelkonen, Department of Orthopaedics, for showing me how to snap microhotos. MSc Axel Tojo, Department of Biomedical Engineering, for the help with the nozzle system. Finally I also want to mention the biomechanics group on floor D13: Lorenzo, Anna, Neashan, Hanifeh and Giacomo.

References

[1] G. Victoria, B. Petrisor, B. Drew, and D. Dick, "Bone stimulation for fracture healing: What's all the fuss?" *Indian journal of orthopaedics*, vol. 43, no. 2, p. 117, 2009.

[2] N. Mathavan, P. Bosemark, H. Isaksson, and M. Tägil, "Investigating the synergistic efficacy of bmp-7 and zoledronate on bone allografts using an open rat osteotomy model," *Bone*, vol. 56, no. 2, pp. 440–448, 2013.

[3] P. Bosemark, C. Perdikouri, M. Pelkonen, H. Isaksson, and M. Tägil, "The masquelet induced membrane technique with bmp and a synthetic scaffold can heal a rat femoral critical size defect," *Journal of Orthopaedic Research*, vol. 33, no. 4, pp. 488–495, 2015.

[4] "Biomechanics group, lth," http://bme.lth.se/research-pages/biomechanics/research/assessment-of-bone-quality/.

[5] A. K. Harding, P. Aspenberg, M. Kataoka, D. Bylski, and M. Tägil, "Manipulating the anabolic and catabolic response in bone graft remodeling: Synergism by a combination of local bmp-7 and a single systemic dosis of zoledronate," *Journal of Orthopaedic Research*, vol. 26, no. 9, pp. 1245–1249, 2008.

[6] "Kirschner wire," https://en.wikipedia.org/wiki/Kirschner_wire.

[7] "Rat nail, risystems," http://www.risystem.com/Standardized_Implant_for_Research/intramedullary_fixation.html.

[8] C. Brandrick, "Artificial medical implants built with 3d printing," http://www.techworld.com/news/personal-tech/artificial-medical-implants-built-with-3d-printing-3335696/, February 2012.

[9] A. Kooser, "3d-printed implant replaces 75 percent of patient's skull," http://www.cnet.com/news/3d-printed-implant-replaces-75-percent-of-patients-skull/, March 2013.

[10] H. Lipson and M. Kurman, *Fabricated: The new world of 3D printing.* John Wiley & Sons, 2013.

[11] C. L. Ventola, "Medical applications for 3d printing: current and projected uses," *Pharmacy and Therapeutics*, vol. 39, no. 10, p. 704, 2014.

[12] "3d printing," http://en.wikipedia.org/wiki/3D_printing#Consumer_use.

[13] E. Sachs, M. Cima, P. Williams, D. Brancazio, and J. Cornie, "Three dimensional printing: rapid tooling and prototypes directly from a cad model," *Journal of Manufacturing Science and Engineering*, vol. 114, no. 4, pp. 481–488, 1992.

[14] K. Modjarrad and S. Ebnesajjad, *Handbook of Polymer Applications in Medicine and Medical Devices.* Elsevier, 2013.

[15] "Bio-flex v-135001 (trial grade)," http://colorfabb.com/files/FKUR/TD_BIO-FLEX_V_135001_en.pdf.

[16] "Polylactic acid (pla, polylactide)," http://www.makeitfrom.com/material-properties/Polylactic-Acid-PLA-Polylactide/.

[17] C. Bozzini, E. O. Picasso, G. M. Champin, R. M. Alippi, and C. E. Bozzini, "Biomechanical properties of the mid-shaft femur in middle-aged hypophysectomized rats as assessed by bending test," *Endocrine*, vol. 42, no. 2, pp. 411–418, 2012.

[18] R. Ritchie, K. Koester, S. Ionova, W. Yao, N. Lane, and J. Ager, "Measurement of the toughness of bone: a tutorial with special reference to small animal studies," *Bone*, vol. 43, no. 5, pp. 798–812, 2008.

[19] "Bridge specifications, industrial uses, faq," http://www.taulman3d.com/bridge-features.html.

[20] C. H. Turner and D. B. Burr, "Basic biomechanical measurements of bone: a tutorial," *Bone*, vol. 14, no. 4, pp. 595–608, 1993.

[21] I. Vroman and L. Tighzert, "Biodegradable polymers," *Materials*, vol. 2, no. 2, pp. 307–344, 2009.

A Blueprints

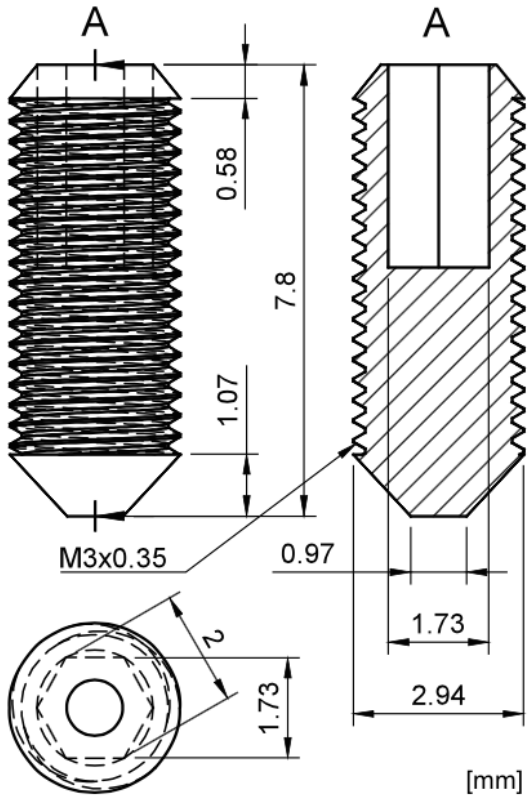

Figure 18: Blueprint of the bone screw.

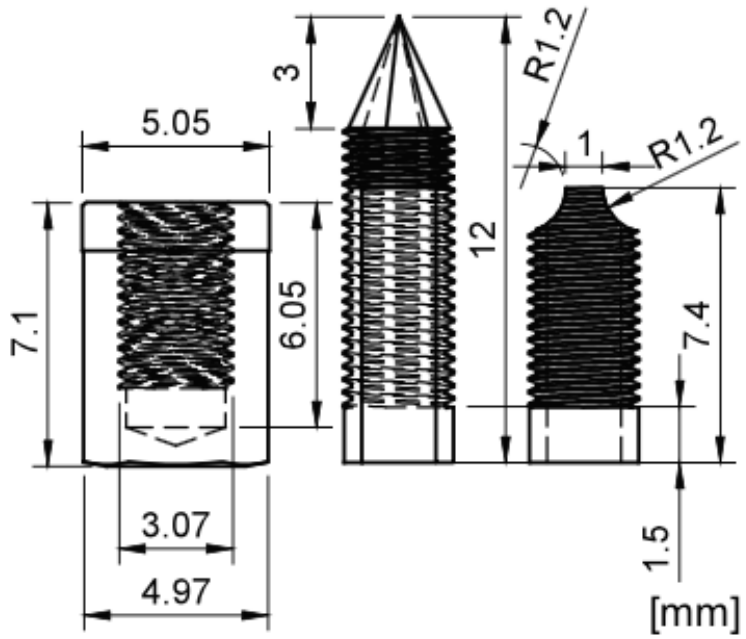

Figure 19: Blueprint of the shielded bone chamber screw.

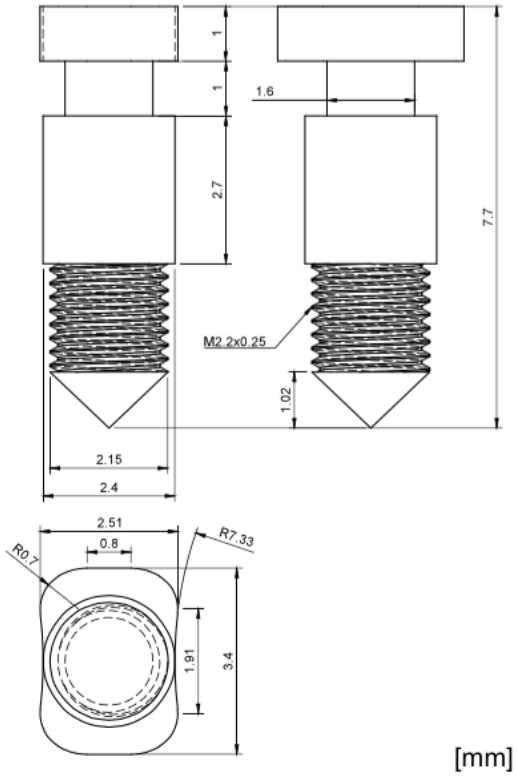

Figure 20: Blueprint of the torque screw.

B Printer settings

Table 2: Printer settings for PLA with a ⌀0.4 mm nozzle. Settings not mentioned were imported from the high settings standard in Cura

Nozzle temp.	210° C	Fill	100 %
Build plate temp.	60° C	Print speed	15 mm/s
Layer height	0.04 mm	travel speed	150 mm/s
Shell Thickness	0.4 mm	bottom layer time, min	5 s
Cooling fan	100 %	Initial layer	0.1 mm
Raft extra margin	1.6 mm	line spacing	0.8

Table 3: Printer settings for PLA with a ⌀0.25 mm nozzle. Settings not mentioned were imported from the high settings standard in Cura

Nozzle temp.	210° C	Fill	100 %
Build plate temp.	60° C	Print speed	15 mm/s
Layer height	0.02 mm	travel speed	150 mm/s
Shell Thickness	0.25 mm	bottom layer time, min	5 s
Cooling fan	100 %	Initial layer	0.1 mm
Raft extra margin	1.5 mm	line spacing	0.75 mm

Table 4: Printer settings for Nylon with a ⌀0.4 mm nozzle. Settings not mentioned were imported from the high settings standard in Cura

Nozzle temp.	245° C	Fill	100 %
Build plate temp.	50° C	Print speed	15 mm/s
Layer height	0.04 mm	travel speed	150 mm/s
Shell Thickness	0.4 mm	bottom layer time, min	5 s
Cooling fan	40 %	Initial layer	0.1 mm
Raft extra margin	1.6 mm	line spacing	0.8 mm

C Nail diameter data

Table 5: Measurements of nail diameters

Measurements: [mm]	1	2	3	4	Mean	SD
PLA Nail ⌀ 1.1 mm, nozzle 0.4 mm						
Nail 1	1.14	1.00	1.09	1.13	1.09	0.06
Nail 2	1.21	0.96	1.08	0.99	1.06	0.05
Nail 3	1.17	1.02	1.02	1.13	1.09	0.07
PLA ⌀ 1.5 mm, nozzle 0.4 mm						
Nail 1	1.55	1.49	1.47	1.58	1.52	0.04
Nail 2	1.43	1.51	1.43	1.53	1.48	0.05
Nail 3	1.58	1.42	1.58	1.6	1.55	0.07
PLA ⌀ 1.1 mm, nozzle 0.25 mm						
Nail 1	1.25	1.27	1.24	1.12	1.22	0.06
Nail 2	1.12	1.13	1.1	1.22	1.14	0.05
Nail 3	1.12	1.25	1.26	1.11	1.19	0.07
PLA in saline, ⌀ 1.1 mm, nozzle 0.4 mm						
Nail 1	1.02	1.11	1.03	1.19	1.09	0.07
Nail 2	1.04	1.14	1.01	1.11	1.08	0.05
Nail 3	1.19	1.23	1.15	1.06	1.16	0.06
Manually extruded PLA						
Nail 1	1.11	1.03	1.09	1.08	1.08	0.03
Nail 2	1.12	1.13	1.11	1.13	1.12	0.01
Nylon, ⌀ 1.1 mm, nozzle 0.4 mm						
Nail 1	1.19	1.13	1.17	1.16	1.16	0.02
Nail 2	1.14	1.08	1.04	1.15	1.12	0.04
Nail 3	1.16	1.15	1.05	1.16	1.13	0.05
Nylon in saline, ⌀ 1.1 mm, nozzle 0.4 mm						
Nail 1	1.15	1.11	1.16	1.17	1.15	0.02
Nail 2	1.18	1.19	1.18	1.20	1.19	0.01
Nail 3	1.21	1.19	1.19	1.12	1.18	0.03

D Material Degradability

Table 6: Relative weight development of PLA/PHA pellets kept at 37° for 15 weeks

Printed at 180° C					
Week	a)	b)	c)	Mean	SD
0	1	1	1	1	0
2	.98	1	1	.99	.01
6	.98	1	1	.99	.01
15	.99	1	1	.99	.01
Printed at 200° C					
0	1	1	1	1	0
2	1	1	1	1	0
6	1	1	1	1	0
15	1.01	1.01	1.01	1.01	0
Printed at 220° C					
0	1	1	1	1	0
2	1	1	.98	.99	.01
6	1	1	.98	.99	.01
15	1.01	1.02	1.00	1.01	.01

Table 7: Relative weight development of PLA/PHA pellets kept at 60° for 15 weeks

Printed at 180° C					
Week	a)	b)	c)	Mean	SD
0	1	1	1	1	0
2	.76	.79	.79	.78	.02
6	.22	.60	.60	.48	.22
15	.08	.15	.29	.17	.01
Printed at 200° C					
0	1	1	1	1	0
2	.80	.78	.79	.86	.12
6	.59	.61	.60	.60	.10
15	.25	.27	.29	.27	.02
Printed at 220° C					
0	1	1	1	1	0
2	.79	.78	.81	.79	.01
6	.58	.59	.62	.60	.02
15	.26	.26	.28	.27	.01

E Microphotos

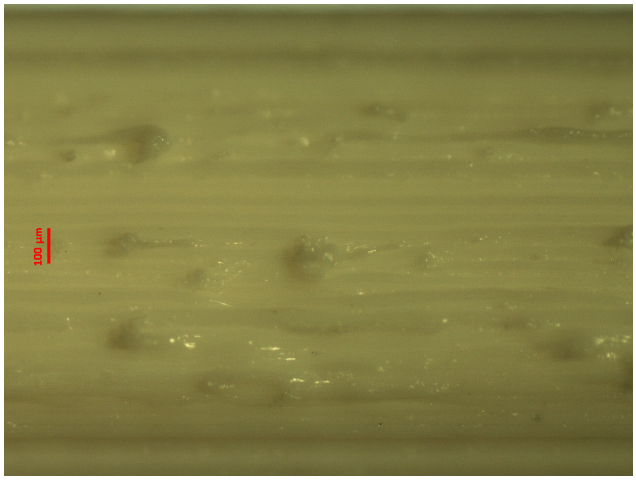

Figure 21: Microscopy of PLA nail side with 1.5 mm diameter printed with the 0.4 mm nozzle from group 2.

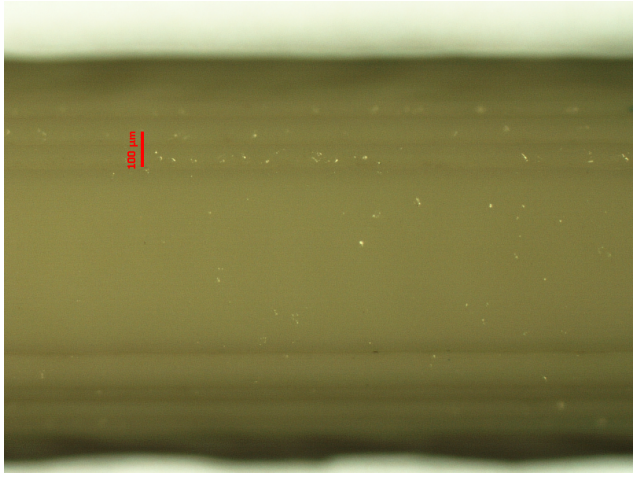

Figure 22: Microscopy of PLA nail top side with 1.1 mm diameter printed with the 0.25 mm nozzle from group 3.

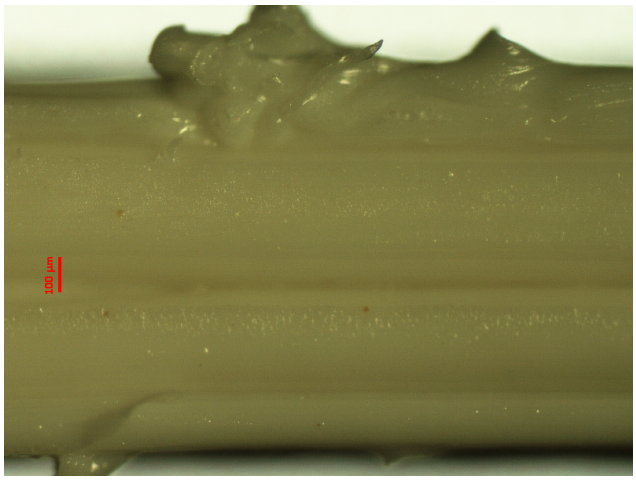

Figure 23: Microscopy of PLA nail underside with 1.1 mm diameter printed with the 0.25 mm nozzle from group 3.

F Force-displacement curves

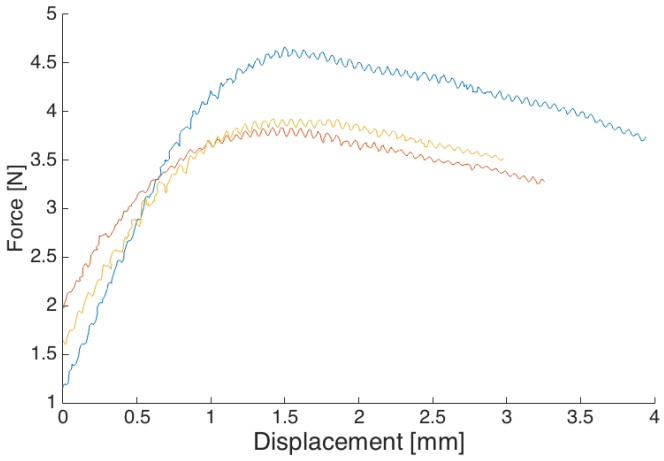

Figure 24: Force-displacement curves from 3 nails from group 1: PLA nails with ⌀1.1 mm printed with ⌀0.4 mm nozzle.

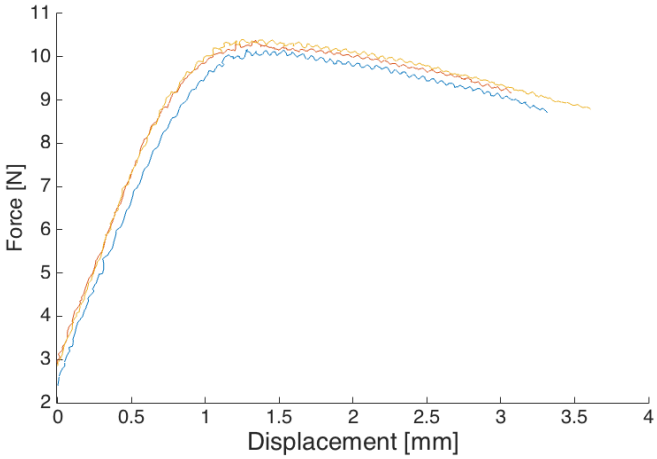

Figure 25: Force-displacement curves from 3 nails from group 2: PLA nails with ⌀1.5 mm printed with ⌀0.4 mm nozzle.

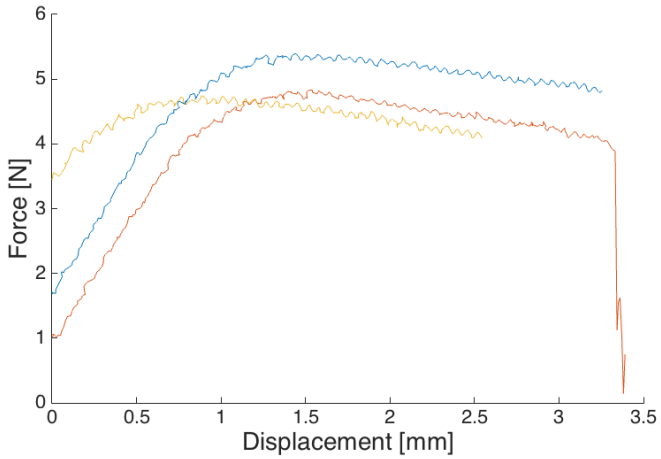

Figure 26: Force-displacement curves from 3 nails from group 3: PLA nails with ⌀1.1 mm printed with ⌀0.25 mm nozzle.

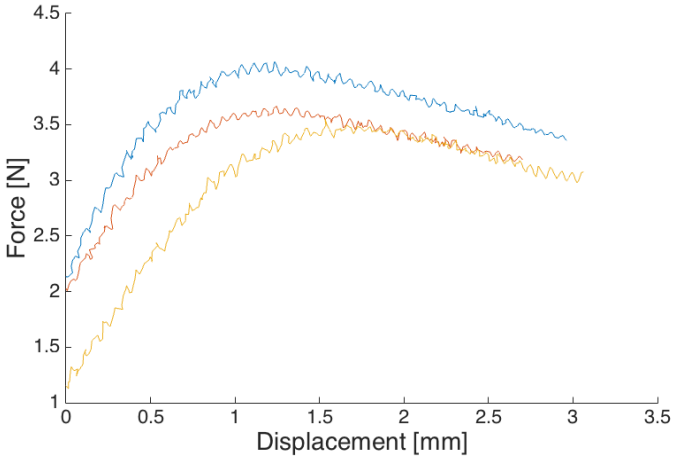

Figure 27: Force-displacement curves from 3 nails from group 4: Wet PLA nails with ⌀1.1 mm printed with ⌀0.4 mm nozzle.

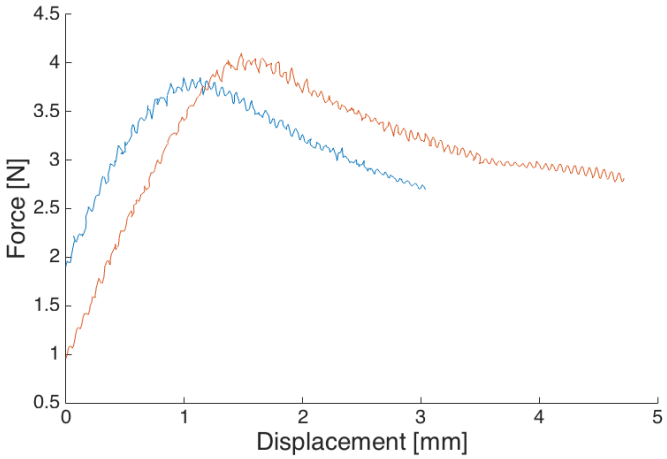

Figure 28: Force-displacement curves from 2 nails from group 5: PLA nails manually extruded through ⌀0.8 mm nozzle.

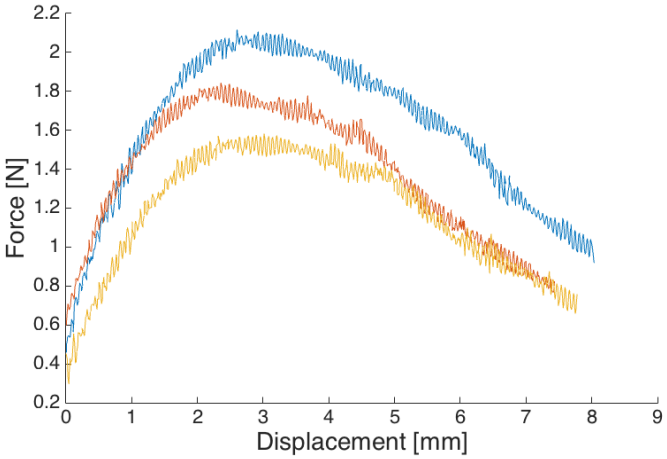

Figure 29: Force-displacement curves from 3 nails from group 6: Nylon nails with ⌀1.1 mm printed with ⌀0.4 mm nozzle.

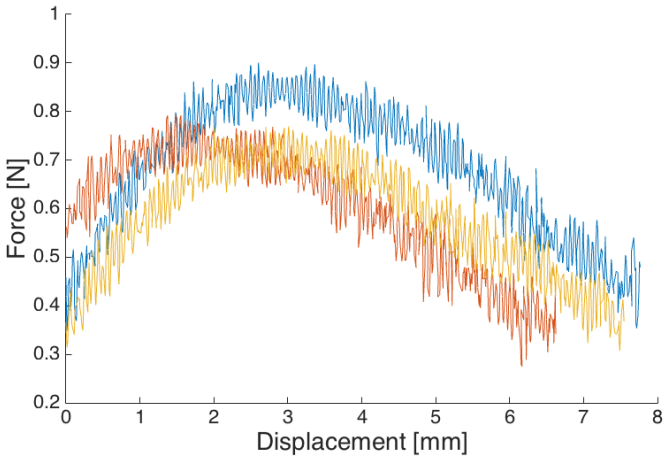

Figure 30: Force-displacement curves from 3 nails from group 7: Wet Nylon nails with ⌀1.1 mm printed with ⌀0.4 mm nozzle.